Measurement of nucleotide exchange kinetics with isolated synthetic myosin filaments using flash photolysis

Paul B. Conibear, Clive R. Bagshaw*

Department of Biochemistry, University of Leicester, Leicester LE1 7RH, UK

Received 10 November 1995; revised version received 22 December 1995

Abstract The kinetics of nucleotide release have been measured at the level of isolated synthetic myosin filaments. This was achieved by displacing a rhodamine nucleotide analog from a filament by flash photolysis of caged-ATP with selective observation using total internal reflectance fluorescence microscopy. The procedure gave improved time resolution over previously used flow methods. Kinetics were measured both in the presence of the ADP analog and during steady-state hydrolysis of the ATP analog. These studies open the way for kinetic measurements during actin filament sliding on myosin tracks.

Key words: Fluorescence microscopy; Motility assay (in vitro); Transient kinetics; Myosin ATPase

1. Introduction

Motor proteins, such as myosin and actin, convert the chemical energy of ATP hydrolysis into mechanical work. A fundamental goal in understanding the mechanism of this process is to determine whether the ATPase activity is tightly coupled to the mechanical cycle of cross-bridge action. To this end, recent effort has been directed towards in vitro motility assays where mechanical events have now been detected at the level of single molecular interactions between actin and myosin [1–3]. Likewise, the sensitivity of ATPase assays have been improved so that the long-lived myosin product complex (M.ADP.P_i) can be detected at the single molecule level [4]. The problem remains, however, of determining the kinetics of the ATPase at this level of sensitivity under conditions of actin activation.

Single molecule mechanical measurements have suggested that the cross-bridge stroke is of the order of 4–17 nm [1–3], which is compatible with the conventional model for the cross-bridge cycle [5]. However, there is no direct evidence of how many such strokes may be derived from the hydrolysis of a single ATP molecule. Under conditions of low load where actin filaments are sliding near their maximum velocity, there remains a discrepancy in the estimation of the distance travelled per ATP molecule hydrolyzed as calculated from bulk assays [6,7].

Previously, we reported the kinetics of ATP turnover by single myosin filaments measured by displacement of a fluorescent ATP analog [8]. In these studies, displacement was achieved by the rapid addition of an excess of ATP using a customised microscope flow cell. The method had a time resolution limited to about 2 s and the signal suffered from the mechanical disturbance occurring during flow and during a temporary pressure change in switching solutions. Nevertheless, the kinetics of displacement were consistent with the reaction monitoring turnover of the ATP analog. Here, we report on modifications to this assay which provide improved time resolution and sensitivity. This lays the foundation for the ultimate goal of simultaneous measurement of actomyosin ATPase activity and mechanical events with single molecular tracks.

2. Materials and methods

2.1. Buffers

Experiments were carried out under the following buffer conditions: 25 mM KCl, 4 mM $MgCl_2$, 1 mM EGTA, 100 mM β-mercaptoethanol, 20 mM imidazole, pH 7.4 at 20°C (microscopy); 40 mM NaCl, 1 mM $MgCl_2$, 20 mM TES, pH 7.5 at 20°C (stopped-flow fluorometry).

2.2. Nucleotides and proteins

2′ (3′)-*O*-[*N*-[2-[3-[5(6)-Tetraethylrhodamine] thioureido] ethyl] carbamoyl]-adenosine 5′ triphosphate (REDA-ATP; Fig. 1) was synthesized by reacting rhodamine B isothiocyanate (mixed 5(6) isomers, Sigma Chemical) with 2′ (3′)-*O*-[aminoethyl carbamoyl]-adenosine 5′ triphosphate under the same conditions described for synthesis of the analogous fluorescein derivative [8]. REDA-ADP was prepared on a small scale by incubation of REDA-ATP (20 μM) with 2 μM myosin subfragment 1 (S1) for 30 min at 20 °C.

Myosin and S1 were prepared from rabbit skeletal muscle as described previously [8]. Synthetic myosin filaments were prepared as follows. Myosin was dissolved at 1 mg/ml in 0.5 M NaCl, 20 mM imidazole, pH 6.8 and subsequently dialyzed against a 100-fold excess of 0.12 M NaCl, 20 mM imidazole, 1 mM DTT, pH 6.8 for 12 h. Prior to an experiment, an aliquot of the dialysate was diluted 20-fold in microscopy buffer and 50 μl applied to an observation cell of dimensions 170 μm × 18 mm × 5 mm [9]. Non-immobilized protein was washed out with a 5-fold excess of microscopy buffer after a 3-min incubation period. We estimate that about 10% of the myosin filaments were immobilized. This was determined both from a direct tryptophan fluorometric assay of the protein washed out of the cell and from the catalytic activity of immobilized myosin with REDA-ATP as a substrate.

2.3. Flash photolysis

Displacement of REDA nucleotides from myosin filaments was achieved by the rapid release of ATP from P^3-1-(2-nitrophenyl)-ethyl adenosine 5′ triphosphate (caged-ATP; Calbiochem Novabiochem, UK) using a XF-10 xenon flashlamp (Hi-Tech Scientific, UK). The flashlamp was modified in two ways to assist in its use with a microscope. First, a light-emitting diode was mounted just behind the xenon flashlamp so that an image of the electrodes could be accurately aligned and focused in the sample plane. Second, the 20-mm focal length (f.l.) objective lens supplied with the flashlamp was replaced with an 8-mm f.l. lens combination (constructed from 3 silica singlet lenses; Comar Instruments, Cambridge, UK) to increase the intensity of the focused spot. The spot size in the focal plane was estimated to be about 0.2 mm based on the image of the electrodes when viewed through the microscope.

2.4. Fluorescence microscopy

Filaments were observed with a Zeiss Axiovert 135TV microscope using the Omega Optical XF37 (rhodamine) filter/dichroic set. Images

*Corresponding author. Fax: (44) (116) 252 3369.

This work is dedicated to the memory of Professor David Gingell who introduced us to total internal reflectance fluorescence microscopy [15].

SSDI 0014-5793(95)01538-8

were recorded using a Hamamatsu C2400–08 SIT camera coupled to an Argus 10 image processor. Individual frames were grabbed with a Scion LG3 card interfaced to a 7100 Macintosh PowerPC. A macro program was written for the NIH image program (Public Domain) to capture a series of frames with a defined dual timebase. At a preset time, an output signal from the LG3 card was used to briefly close a protective electronic shutter (Ealing Electro-Optics; 22–8411) in front of the camera and to trigger the flash lamp. The shutter reopened within 10–20 ms of the flash. Subsequent to capture of the image stack, regions of interest were defined around a filament and their average pixel intensities were computed as a function of time. The data were transferred to Kaleidagraph (Synergy Software) for data processing, plotting and non-linear least-squares fitting.

In order to selectively excite REDA nucleotides bound to the immobilized myosin, a modification of the total internal reflectance fluorescence (TIRF) method of Stout and Axelrod [10] was used. The optical layout (Fig. 2) accommodates a modification for the Zeiss infinity-corrected optics and avoids the need for precise machining of a black disc to a fixed size. This method produces an annulus of light at N.A. 1.33–1.4 in the back focal plane (BFP) which is totally internally reflected at the coverglass-solution interface. Thus, excitation occurs predominantly via an evanescent field which has a limited penetration depth of the order of 200 nm.

2.5. Stopped-flow fluorometry

Solution kinetics were performed using a SF17MV stopped-flow apparatus [8,11] equipped with a Hg-Xe arc lamp (Applied Photophysics, Leatherhead, UK). Rhodamine was excited at 546 nm and the emission monitored with a 580-nm-long pass filter.

3. Results

Myosin filaments may be observed by fluorescence microscopy upon perfusion with fluorescent nucleotide analogs. The

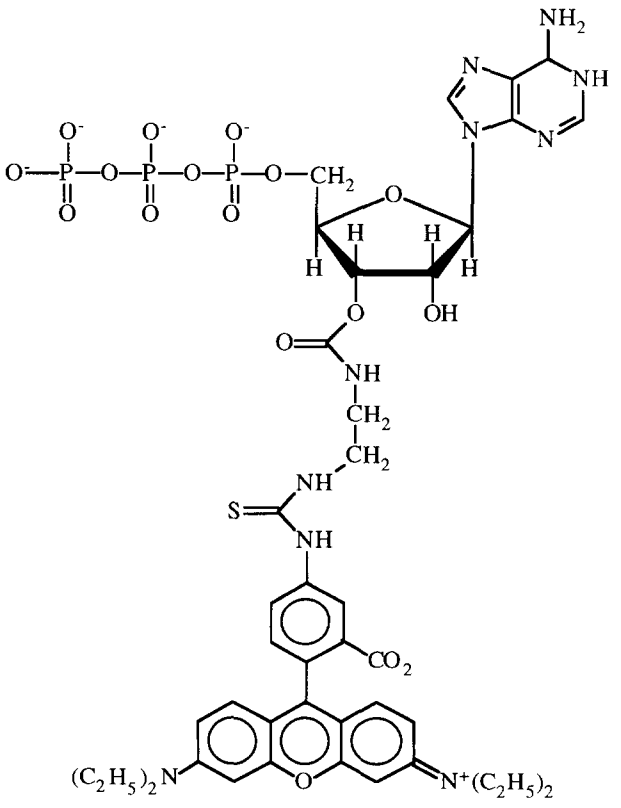

Fig. 1. The structure of REDA-ATP. The sample comprises positional isomers with respect to the 2′ and 3′ ribose ring and 5 and 6 position of the rhodamine.

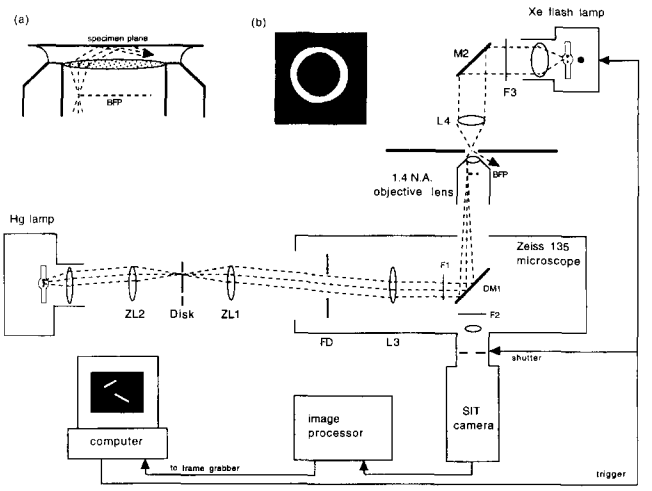

Fig. 2. The optical layout of the microscope. Fluorescence was excited using off axis rays selected by means of a 5-mm black metal disk mounted in apposition with an iris diaphragm. The disk was positioned at the focal plane of a 80–200-mm f.l. camera zoom lens and image of the disk was brought into focus at the BFP of a 63 × oil-immersion 1.4 N.A. microscope objective by operating ZL1 in conjunction with the microscope epitube 100-mm f.l. lens (L3). The disk was illuminated with a Hg lamp. The image of the arc was focused at the black disc with a second zoom lens (ZL2) and the magnification was adjusted so that the disc could be efficiently illuminated without overfilling the back of the objective. For Köhler illumination of the sample plane, the arc lamp image was focused on the disk. Inset (a) shows details of the ray diagram in the region of the objective. Excitation light was brought to focus at the BFP where the peripheral rays corresponding to an N.A. of >1.33 were selectively transmitted. The dashed line (----) represents the image of the disk at the BFP which blocks the central rays. Inset (b) shows an experimental image recorded at the BFP as observed with a Bertrand lens. The size of the annulus of light depends on the ratio of focal lengths of ZL1 to L3 and was adjusted using the zoom control and the iris surrounding the disk. Rays emanating from the objective lens at N.A. >1.33 approach the coverglass-solution interface of the specimen plane at super critical angles and undergo total internal reflectance. Fluorescence was recorded with the SIT camera through standard barrier filters (F1, F2) and dichroic mirror (DM1) assembly. Photolysis was induced using a Xenon flash lamp with a UG11 filter (F3) selecting 360 nm light. For convenience of use, a silica 8-mm f.l. objective lens (L4) was mounted on the microscope condenser holder and aligned and focused using the field diaphragm of the microscope condenser assembly. A 45° front-surfaced U.V. mirror was then introduced and the Xe arc lamp electrodes aligned with the aid of a light-emitting diode mounted on axis behind the Xe arc lamp (●). With a 10 × objective lens, the image of the Xe arc electrodes could be observed at the specimen plane.

filaments fluoresce above the background signal because of the local high concentration of nucleotide bound to the myosin heads [8]. Although rhodamine has a lower quantum yield than fluorescein, we found that the use of REDA-ATP as a substrate gave better contrast than for the corresponding fluorescein analog, possibly because the former is less susceptible to photobleaching. Transient kinetic studies suggest these analogs are comparable with ATP in their interaction with S1 in solution [11]. For microscopy, we used a concentration of REDA-ATP of 200 nM. This is close to the K_m and, thus, represents a compromise between attaining a measurable signal from the bound analog and minimizing the relative contribution from the free analog in the bulk solution. By using the TIRF method, further improvement in contrast was achieved. Synthetic myosin filaments were observed as 10–30 μm aggregates often

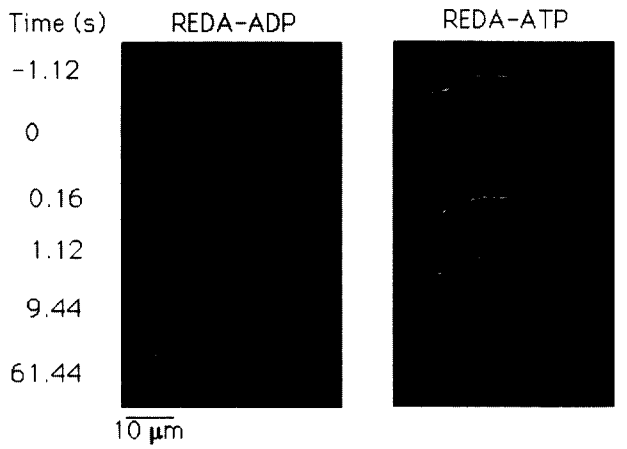

Fig. 3. Montage showing the displacement of REDA nucleotides induced by flash photolysis of caged-ATP. Immobilized myosin filaments were incubated with 200 nM REDA-ADP + 100 μM caged-ATP and subjected to a U.V. flash. After the displacement was complete, the preparation was flushed through with 200 nM REDA-ATP in place of the REDA-ADP and subjected to a second U.V. flash.

visibly fraying into two or three duller and thinner strands at their ends (Fig. 3). In the central part, filaments typically fluoresce at approximately 60% above the background. The molecular density of these structures is difficult to define precisely because of uncertainty in the degree and pattern of aggregation. However, native clam filaments which are structurally better defined gave fluorescence intensities comparable to the rabbit aggregates. Thus, by comparison with native clam filaments [8], we estimate that the molecular density is 1000–2000 myosin heads per μm for the rabbit aggregates and therefore a few hundred heads per μm for the duller strands. The latter is comparable to that of native rabbit filaments.

Displacement of the fluorescent nucleotide was achieved by flash photolysis of caged-ATP. We estimate that about 20% of the caged-ATP was broken down by a single flash. At 100 μM caged-ATP, this was sufficient to effect complete displacement. Fig. 3 shows representative images of myosin filaments from an experiment in which caged-ATP was photolyzed first in the presence of REDA-ADP and then in the presence of REDA-ATP. The timecourse of fluorescence decay is clearly faster in the case of REDA-ADP. This fast process is attributed to dissociation of the M.REDA-ADP state. By analogy with ATP itself, the slower process observed with REDA-ATP is attributed to P_i-release from the M.REDA-ADP.P_i which limits the overall turnover rate. Quantitative analysis of such intensity changes yields rate constants of 0.77 s^{-1} (REDA-ADP; Fig. 4b,d) and 0.06 s^{-1} (REDA-ATP; Fig. 4a,c). These values compare well with those obtained by stopped-flow experiments with S1 in solution of 0.5 s^{-1} (see below) and 0.03 s^{-1} [11], respectively. On prolonged incubation (>10 min) with REDA-ATP, the displacement showed biphasic kinetics in line with the exhaustion of substrate and a build up of product REDA-ADP in the bulk solution. The data shown (Fig. 4) were obtained by analysis of a 5-μm segment of the thicker central part of the bundle. The kinetics of displacement could still be followed, albeit with reduced signal-to-noise, when comparable and shorter (1 μm) lengths of the thinner strands were selected.

Similar kinetics were obtained when the same filament was subjected to displacement by photolysis of caged-ATP for at least 3 × and the results were independent of whether the filaments were perfused first with REDA-ATP or REDA-ADP. Thus, the loss of catalytic function resulting from the U.V. flash is minimal. Displacement of the fluorophore after a flash was complete, so that the final filament and background intensity were indistinguishable, suggesting photosensitized cross-linking of the fluorophore was negligible [12]. Control flashes in the absence of caged-ATP, together with flashes in the presence of caged-ATP with filaments on which REDA nucleotide was a trapped as a stable ternary M.REDA-ADP.AlF_4^- complex [11], showed that photobleaching of both bound and free REDA-ATP was negligible (<1%; data not shown). Thiol reagents (70–100 mM β-mercaptoethanol) were generally included as a precautionary measure but were not essential. There was no indication of phosphorescence from the coverglass or immersion oil on the timescale investigated (0.1–60 s). The absence of the above artefacts is in line with an absence of any fast phase upon flash photolysis in the presence of REDA-ATP (Fig. 4c).

The major problem associated with the current use of flash photolysis results from the fact that caged-ATP is a weak competitive inhibitor of ATP binding [13]. This causes partial displacement of the fluorescent ATP analog prior to photolysis. 100 μM caged-ATP results in a decrease in image intensity of 60% and images could still be observed at 1 mM caged-ATP. Any contaminant ADP or ATP in the caged-ATP preparation, or photogenerated under the microscope, will contribute to this competition, although we have found that pretreatment with hexokinase and/or apyrase did not alleviate the displacement. In any event, competition from either source with REDA nucle-

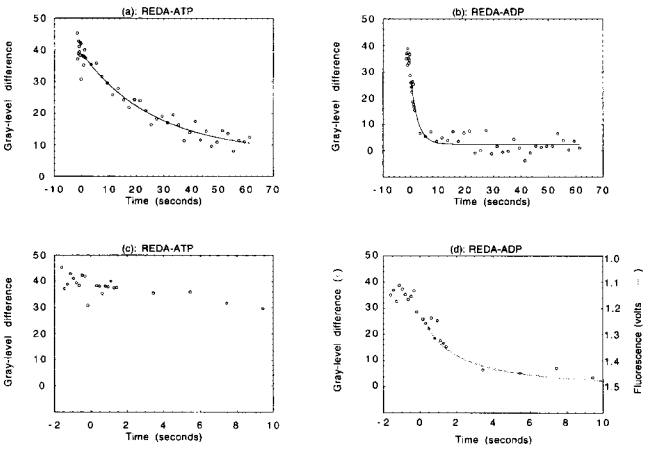

Fig. 4. Quantitative analysis of the displacement of REDA nucleotides. The protocol was similar to that of Fig. 3 except that the sample was subjected to a flash first in the presence of REDA-ATP (a,c) and subsequently in the presence of REDA-ADP (b,d). 5-μm segments were analysed comparable in thickness to the thickest part of the filament shown in Fig. 3. In a and c, data are plotted for all 50 of the grabbed frames. Fitted lines to single exponentials are superimposed, giving rate constants of 0.06 s^{-1} for REDA-ATP and 0.77s^{-1} for REDA-ADP. In b and d, only data from the early frames are shown. Gray-level difference values (○) were calculated as average gray levels of a filament segment minus those of a segment from the background to correct for minor global intensity changes of the field. The dark-level difference corresponds to an average value of −69 for REDA-ATP and −83 for REDA-ADP. (d) Includes scaled data from a stopped-flow experiment showing the increase in rhodamine fluorescence when 2 μM REDA-ADP was displaced from a complex with 10 μM S1 by rapid mixing with 50 μM ATP [11].

otides is likely to effect only the amplitude rather than the kinetics of observed intensity changes.

The REDA-ADP-dissociation kinetics provide a test of the time resolution of the apparatus. Fig. 4d shows the displacement of REDA-ADP from a myosin filament compared with a stopped-flow record obtained in solution with S1. This close correspondence suggests that reactions can be reliably monitored in this time window. The limiting factor in the current photolysis experiment is the response time of the SIT camera which, at high gains, shows a persistence of about 100 ms.

4. Discussion

The use of flash photolysis has given an order of magnitude gain in time resolution over the previous flow technique used by Sowerby et al. [8]. As a consequence, we can now monitor displacement from a 1-μm segment of a synthetic myosin filament estimated to contain a few hundred sites with a time resolution of 0.1 s. Furthermore, the technique has made records much more reproducible owing to the lack of mechanical artefacts inherent to flow methods. The finding that ATP can be released photolytically without damage to the catalytic activity of myosin is a necessary prerequisite for the general use of flash photolysis and bodes well for studies using caged fluorescent ATP analogs [14]. We have initiated the sliding of actin in in vitro motility assays with this apparatus [15], but this process is more susceptible to damage from the free radicals released during photolysis and inclusion of thiol reagents is essential. The main drawback to the use of caged-ATP is its competitive inhibition [13]. Although this does not pose problems at the 100 μM concentrations used in the present work, the signal-to-noise ratio is considerably impaired at the mM concentrations required to support sliding at maximal velocity in an in vitro motility assay. Increasing the local degree of photolysis by using a U.V. laser may permit the use of lower caged-ATP concentrations.

Analysing the average intensity of pixels corresponding to a segment of the imaged filament has an advantage over the photomultiplier detection system used previously [8], in that unwanted light from the surrounding area is reduced. However, the use of a photomultiplier offers faster time resolution than standard video technology. Use of a photomultiplier in conjunction with a pinhole may be the best option for both good time resolution and optimum spatial selectivity.

The optical layout used here has provided some increase in contrast over conventional epi-illumination although considerably less than expected in theory. The gain in contrast is limited by stray light entering the objective at subcritical angles. Further improvements could be achieved with the more favourable beam characteristics from a laser [10] and dichroic mirrors that reflect a maximal proportion of the incident light [4]. However, compared with the prism-based method [4,15], TIRF via the objective lens allows an optimal objective-to-specimen working distance as well as free access to the opposite surface for the photolysis beam.

We have also used REDA-ATP to follow nucleotide turnover in single myofibrils which contract isometrically or auxotonically against glass microneedles [16]. Interestingly, in isometric conditions and at long sarcomere lengths where the bulk of the myosin cannot interact with actin, the observed rate of displacement following photolysis of caged-ATP was faster than that expected for the dissociation of the M.REDA-ADP.P_i state, and indeed was close to that for the M.REDA-ADP state. This situation probably arises because at the low concentrations of REDA-ATP used in the bathing solution (200 nM), there is a depletion of REDA-ATP in the myofibril lattice and a build up of REDA-ADP because the local myosin concentration is around 200 μM sites. Increasing the REDA-ATP to 5 μM reduced this problem and gave a phase of displacement with a rate constant comparable to that observed here for the M.REDA-ADP.P_i state. In this case, confocal microscopy was used to resolve the A-band staining pattern from the high background fluorescence from REDA-ATP in the bulk solution [16].

Finally, we would like to point out that, although single molecule detection has been reported and opens up new possibilities with regard to mechanochemical coupling studies of motor proteins [4], the major discrepancies in the literature concern sliding over assemblies of myosin heads at low loads [6,7]. Thus, it may be desirable to follow the kinetics of nucleotide turnover by a few hundred adjacent myosin heads during unloaded sliding. In such assemblies, single molecules could not be resolved at the level of light microscopy. The use of flash photolysis to initiate nucleotide exchange in small assemblies therefore represents a relevant approach to the problem and one that is complementary to stochastic kinetic analysis of individual molecules.

Acknowledgements: We are grateful to Charnjit Seehra and Mick Lee for the synthesis of REDA-ATP, and Tony Smith and Mac Callender for engineering lens mounts. We are grateful to Dan Axelrod for discussions on TIRF. This work was supported by the Wellcome Trust. The flashlamp was purchased under the Molecular Recognition Initiative of the BBSRC.

References

[1] Finer, J.T., Simmons, R.M. and Spudich, J.A. (1994) Nature (London) 368, 113–119.
[2] Molloy, J.E., Burns, J.E., Kendrick-Jones, J., Tregear, R.T. and White, D.C.S. (1995) Nature (London) 378, 209–212.
[3] Ishijima, A., Harada, Y., Kojima, H., Funatsu, T., Higuchi, H. and Yanagida, T. (1994) Biochem. Biophys Res. Commun. 199, 1057–1063.
[4] Funatsu, T., Harada, Y., Tokunaga, M., Saito, K. and Yanagida, T. (1995) Nature (London) 374, 555–559.
[5] Bagshaw, C.R. (1993) Muscle Contraction. Chapman and Hall, London, UK.
[6] Uyeda, T.Q.P., Kron, S.J. and Spudich, J.A. (1990) J. Mol. Biol. 214, 699–710.
[7] Harada, Y., Sakurada, K., Aoki, T., Thomas, D.D. and Yanagida, T. (1990) J. Mol. Biol. 216, 49–68.
[8] Sowerby, A.J., Seehra, C.K. Lee, M. and Bagshaw, C.R. (1993) J. Mol. Biol. 234, 114–123.
[9] Kron, S.J. and Spudich, J.A. (1986) Proc. Natl. Acad. Sci. USA 83, 6272–6276.
[10] Stout, A.L. and Axelrod, D. (1989) Appl. Optics 28, 5237–5242.
[11] Conibear, P.B., Jeffreys, D.S., Seehra, C.K., Eaton, R.J. and Bagshaw, C.R. (1996) Biochemistry in press.
[12] Hiratsuka, T. (1985) J. Biochem. (Tokyo) 97, 71–78.
[13] Thirwell, H., Sleep, J.A. and Ferenczi, M.A. (1995) J. Muscle Res. Cell Motil. 16, 131–137.
[14] Jeffreys, D.S., Eaton, R.J. and Bagshaw, C.R. (1995) Biochem. Soc. Trans. (London) 23, 401S.
[15] Conibear, P.B., Seehra, C.K., Bagshaw, C.R. and Gingell, D. (1995) Biochem. Soc. Trans. (London) 23, 400S.
[16] Chaen, S., Shirakawa, I., Bagshaw, C.R. and Sugi, H. (1995) Biophysics (Jpn. Biophys. Soc.) 35, S211.